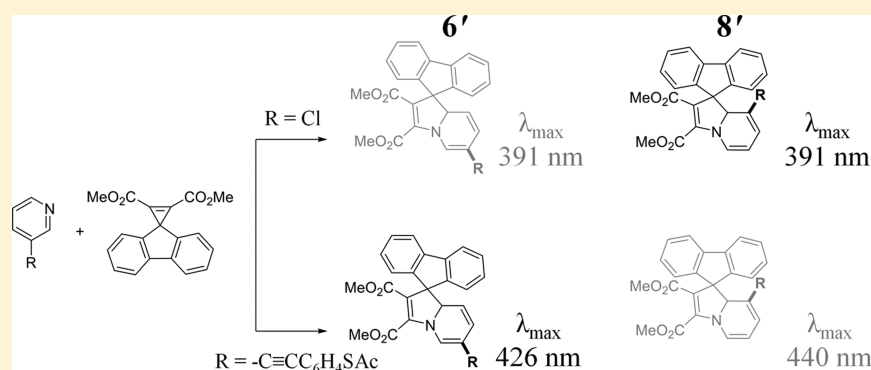


Substituent Parameters Impacting Isomer Composition and Optical Properties of Dihydroindolizine Molecular Switches

Matthew A. Bartucci and Jacob W. Ciszek*

Department of Chemistry and Biochemistry, Loyola University Chicago, 1032 West Sheridan Road, Chicago, Illinois 60660, United States

S Supporting Information



ABSTRACT: In an attempt to understand which factors influence constitutional isomer control of 6'- and 8'-substituted dihydroindolizines (DHIs), a series of asymmetric pyridines was condensed with dimethyl spiro[cycloprop[2]ene-1,9'-fluorene]-2,3-dicarboxylate. The substituents on the pyridial derivatives ranged from donating to withdrawing and demonstrated control over the isomeric ratios for all DHIs. Substituent control proved to be selective for the highly donating amino, which exclusively formed the 8' isomer. The same ratios were reproduced via photolytic experiments, which suggested that the condensation reaction is dominated by the product's thermodynamic stability. The electronic influences of the substituents extends beyond isomer control, as it impacts the DHIs' optical properties and electrocyclization (switching) rates to the spiro conformers. Our results allow us to predict the syntheses and properties of future 6'- or 8'-substituted DHIs, molecules that will be applied in understanding the role of the dipole vector orientation to work function switching.

INTRODUCTION

Photochromic molecules have often been discussed in the context of smart electronics, with the photochromophore acting as a stimuli-responsive switch or trigger.¹ Toward that end, photochromophores have been recently demonstrated to alter the work function of a material in response to incident light.^{2–5} The correlation between molecular change and the work function shift has even been demonstrated.⁵ This effect, if incorporated into an organic thin-film transistor or organic light-emitting diode configuration, could control the device's function. In this scenario, the photochromophore is at the contact point of the leads and the bulk organic species, allowing for tuning of the device's contact resistance.^{6–12}

Within these light-driven molecular switch systems, there are questions that remain (e.g., distance dependence of switching, the amount of free volume needed for a switch to occur, etc.).^{13–15} Of particular importance is demonstrating the relationship between the dipole of the molecule and the surface's work function change. On the basis of our recent work function modulation data,⁵ it would be ideal to build photochromophores that, when irradiated, have their respective dipoles aligned at varying angles to the surface normal. Such

molecules would allow us to confirm the direct correlation between the normal component of the molecular dipole and the change in the work function.

We explore this relationship via a particular class of photochromophores: dihydroindolizines (DHIs).^{16,17} DHIs are advantageous because of their ease of synthesis and array of substitution patterns, which are ideal for tuning their photochemical properties. More importantly, these same substitutions can be used to tether the molecule to the surface (R, Figure 1)⁵ and, depending on their position, control the orientation of the molecular dipole relative to the surface normal. Typically, monolayers on gold are oriented about 30° with respect to the surface normal,¹⁸ and based on the alkyl tethers of our previously studied 7'-substituted DHIs,⁵ a dipole moment ~28° from the surface normal was presumed. To reorient the zwitterion dipole vector, the tether location on the DHI can be relocated to the 6' position, which should generate a dipole nearly parallel to the surface normal after irradiation (based on the most stable packing structures).^{19,20} Other

Received: April 1, 2014

Published: June 11, 2014

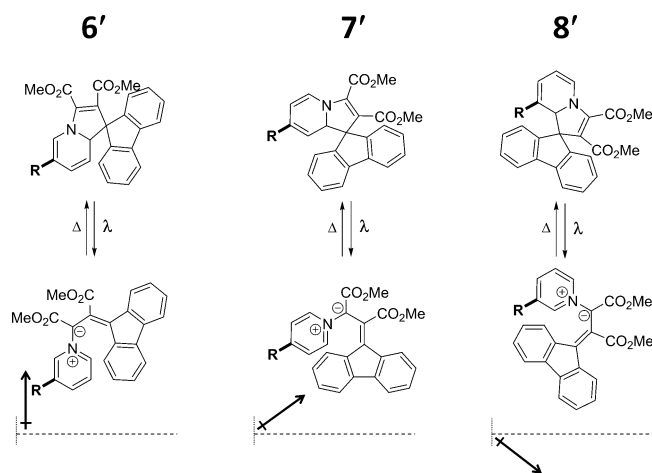


Figure 1. Conformers of DHI, photoisomerization to the betaine form, and orientation of the betaine dipole. The dipole vector, which is relevant for surface/device applications, is indicated with respect to the expected surface normal (dashed line) for molecules tethered to a surface via substituent R. As the location of the tether is moved, so does the corresponding zwitterion dipole orientation with respect to the surface normal.

substitutions, such as 8', would generate a similarly oriented dipole to that of 7' and thus serve as an effective positive control molecule.

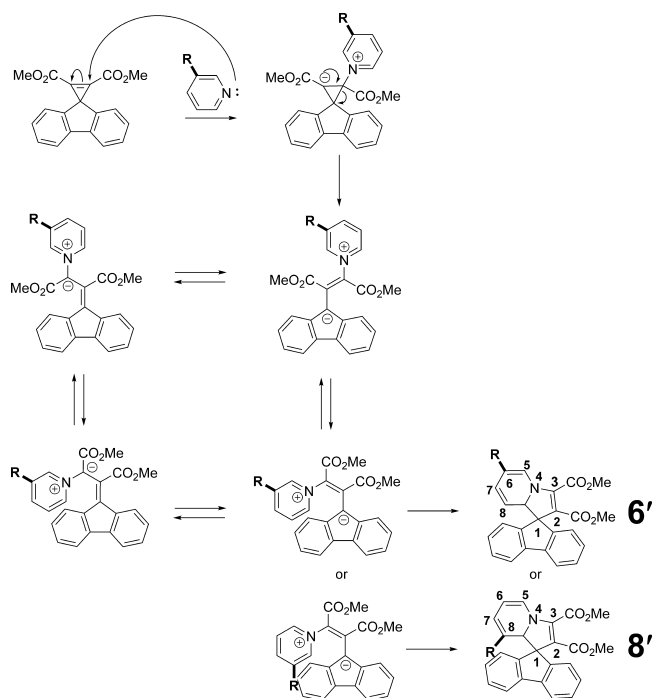
With these substitutions in mind, the synthetic route to generate the asymmetric DHIs leads to an interesting challenge. Because of the reaction pathway, a mixture of the spiro 6' or 8' isomers can be formed via synthesis from 3-substituted pyridines, but the rules for isomer selectivity are not initially obvious; in fact, the isomers have been generated only once before.²¹ However, insight as to what controls the isomer population may be gleaned by correlating the mechanism of formation to substituent effects. Moreover, the changes described above also impact the optical properties of these photochromophores, which are strongly influenced by the electron-donating or -withdrawing capacities of these substituents, adding a second factor to the molecular design.^{22–24}

To elucidate the cause of selectivity over constitutional isomers, we have synthesized a series of asymmetric DHIs and shown a relative trend toward formation of the 6' isomer as the pyridial substituent (R) becomes more electron withdrawing. We show that this can be readily explained via the thermodynamic stability of the parent diene system. Although more complex in origin, perturbation of this diene system also provides justification for changes in absorption maxima locations and intensities. Half-lives track similarly with isomer formation and electron withdrawal, but they stem from resonance stabilization of the pyridinium. We discuss these results as well as the implications for switch design herein.

RESULTS AND DISCUSSION

Structural Isomer Formation. The target compounds are generated via a condensation reaction between dimethyl spiro[cycloprop[2]ene-1,9'-fluorene]-2,3-dicarboxylate and the appropriate 3-substituted pyridine (Scheme 1). The reaction mechanism begins via nucleophilic addition of the pyridine to the spirocyclopropene, generating a cyclopropyl anion. From there, the unstable three-membered ring opens to afford the *trans* isomer of the zwitterion, and the local negative charge can resonate between the C₁ and C₃ atoms.²⁵ Once the zwitterion

Scheme 1. Mechanism of the Condensation Reaction Using a 3-Substituted Pyridine To Afford the 6' and/or 8' DHIs

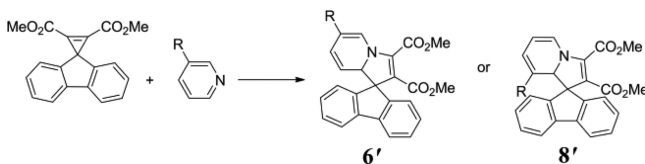


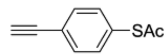
has formed, it resides in the *trans* form because once the *cis* isomer is generated, formation of the 6' or 8' spiro species is rapid.²⁵ However, if the substituents on the pyridinium ion actively donate or withdraw electron density to the positive reaction center, the speed of the electrocyclization is altered and has been correlated with their respective Hammett parameters, showing a linear tendency.^{22,24} More germane to the formed product(s), there is little within this mechanism to suggest selectivity of one geometric isomer over the other as, for example, transition state stabilization ortho to the substituent rather than para is expected to be comparable. In fact, the only obvious means for selecting between 6' and 8' isomers is steric effects.

On the basis of mechanistic arguments, we hypothesize that the pyridial substituents (R) affect the ratio of the 6' and 8' isomers primarily by thermodynamic considerations via the Hammond postulate.²⁶ To test this, substituents that vary in their electronic-directing capabilities were incorporated at the 3-position, from the highly donating amino to the withdrawing acetyl. Furthermore, these pyridine derivatives were selected because of the commercial availability of the pyridine starting materials and the ease of synthesis of the oligo(phenylene ethynylene) (OPE) (Supporting Information, Scheme S1).²⁷ As noted before,²⁷ the formation of the DHIs is facile, and the reaction progress is visually obvious. The seven substituents that were examined (DHIs 7–13, Table 1) follow a loose trend: as the R group becomes more electron withdrawing, the percentage of the 6' spiro isomer is increased. Of these, only the aminopyridine forms exclusively one product (8'), and it was rare to form the 6' in excess, even with acetyl substitution. We were slightly surprised at the different ratios for the iodo and chloro species, especially as the iodo favored the more sterically hindered 8'. However, overall the general electro-negativity trend was consistent.

To facilitate analysis, several experiments were performed in order to examine whether the isolated products were indeed a

Table 1. Yields and Isomer Ratio of Targeted DHIs



DHI	R	Isomer Ratio (6' : 8')	Yield (%)
7	NH ₂	0 : 100	86
8	MeO	7 : 93	83
9	Me	16 : 84	61
10	I	20 : 80	67
11	Cl	30 : 70	57
12		55 : 45	92
13	COCH ₃	63 : 37	79

thermodynamic result. We attempted to interconvert between conformers thermally, but unfortunately, the barrier to interconversion is sufficiently high: pure **DHI-11** (either the 6' or 8' conformers) heated at 50 °C for 15 min show no observable interconversion via their ¹H NMR spectra. As an alternative experiment, several of the DHIs were instead interconverted photolytically ($\lambda = 405$ nm), and in all experiments, the observed ratios were the same (within 10%) as the ones generated during the condensation (Table 1). Compounds examined in this manner include 8'-**DHI-8**, 8'-**DHI-13**, and a 7:3 mixture of 6'/8' **DHI-13** (Supporting Information, Figures S1–S3). In addition, when the condensation was monitored as a function of time via ¹H NMR spectroscopy, the isomer ratio was consistent and unaltered as the reaction progressed.

A thermodynamic explanation for the isomer distributions in Table 1 can be primarily described using the parent diene system as a model (Figure 2), a valid assumption because the

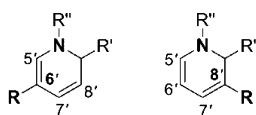


Figure 2. Parent diene system for 6'- and 8'-substituted DHIs. The R' and R'' groups denote the 2,3-dihydropyrrole ring and are identical in the two systems.

positions of the remaining substituents are identical. Control stems from the location of the amine with respect to the R group, either via a shared double bond or distal. Restated, in the case of the 6' conformer (Figure 2, left), both substituents have a resonance and inductive effect on the same bond, and in the case of 8' (Figure 2, right), the interactions are via conjugation. Thus, it is not surprising that for an electron-donating substituent, the additional electron density is best stabilized at the distant 8' position. In the case of a withdrawing group,

substitution at the 6' position generates a stabilized push–pull olefin and is the more favored isomer.²⁸

It can be argued that if isomeric selectivity trends track with electron-withdrawing ability, one should consider the possibility that the effect is from the stabilization of the pyridinium in Scheme 1. We discount this possibility for three reasons. First, the aforementioned experiments suggested that we are observing thermodynamically determined mixtures. Second, invocation of the pyridinium does not provide justification of the observed ratio of 6' to 8'. Finally, no significant solvent effects are observed, suggesting minimal impact of a charged transition state (Supporting Information, Figure S4). It is also worth mentioning that orbital control²¹ or other kinetic sources could be invoked to explain the isomer distribution; however, these are clearly heavily intertwined with the thermodynamics, and attempts to differentiate them would not be meaningful.

Optical Properties. The characteristic feature in the optical absorptions for the DHIs is the π to π^* transition, the same excitation responsible for initiating the molecular switch. We have measured the λ_{\max} for **DHIs 7–13** (Table 2, Figure 3) to study substituent effects. The underpinnings of the transition reside within the same diene system responsible for determining isomeric distributions, and these can be classically analyzed via substituent effects within Woodward–Fieser rules. Specifically, methyl substituents are expected to red shift the parent diene absorption maximum by approximately 5 nm²⁹ (the unsubstituted DHI absorbs at 386 nm). The source of the shift is understood to be purely inductive, as mesomeric effects are inapplicable to the saturated carbon.³⁰ Other simple substituents such as chloro, methoxy, iodo, and amino are only slightly more complex, involving both mesomeric and inductive influences ($\Delta\lambda_{\max} = 5, 4, 13,$ and 25 nm respectively; Table 2 and Figure 3a); all are consistent with predicted shifts.³¹ The more substantial shifts in the case of the iodo species (compared to that of the chloro) arise from a change in the nature of the optical excitation; in the case of the iodoethylene, the I(5p_⊥) is now the highest energy occupied orbital and thus the lowest energy transition for these systems is now the n to π^* transition.^{32,33} The larger shift for the amino group (when compared to those for the chloro and iodo) stems from larger mesomeric effects associated with lone pairs in period two elements.³⁰ In all instances, the position of the substituent on the diene (i.e., 6' vs 8') has a negligible effect on λ_{\max} (Figure 3b), again mirroring experimental trends.³¹

The unsaturated substituents of **DHI-12** and **-13** require explicit discussion, as two different effects must be considered for the additional π systems. The first component is the extension of conjugation, which can be modeled via the free electron model (or MO theory for a more rigorous discussion). Here, it is expected that the absorption maximum will red shift with some proportionality to the length of the system/number of electrons.³⁰ The second component is the effect of cross-conjugation, which is present in systems containing two partially overlapping conjugated systems.³⁴ For cross-conjugated systems, the longest linear system is generally the primary determinant of the lowest energy of absorption, with minor contributions from the cross-conjugation.³⁵ These effects allow us to interpret the absorption spectra of OPE-substituted DHIs, where the substituent is at the 6' (6'-**DHI-12**), 7' (**DHI-1**),²⁷ and 8' (8'-**DHI-12**) positions (Figure 4a). The simplest system is that of 8'-**DHI-12**, where continuous conjugation extends from the diene, through the ethynylene, and beyond (Figure 4b). As this molecule contains no cross-conjugation, it

Table 2. Optical and Half-Life Data for DHIs 7–13

DHI	R	6'		8'		zwitterion λ_{\max} (nm)	$t_{1/2}$ (s)
		λ_{\max} (nm)	$\epsilon \times 10^{-3}$ ($M^{-1} \text{ cm}^{-1}$)	λ_{\max} (nm)	$\epsilon \times 10^{-3}$ ($M^{-1} \text{ cm}^{-1}$)		
7	NH ₂			411	6.2	573	120
8	MeO			390	7.2	581	120
9	Me			390	12	587	51
10	I	397	12	399	10.	606	19 ^a
11	Cl	391	9.0	391	8.0	594	45 ^a
12	OPE	426	38	440	17	596	14 ^a
13	Ac	404	13	433	5.0	594	2.1 ^a

^aAll half-lives under 50 s were the average of two trials monitoring the decay of the zwitterion absorption after excitation.

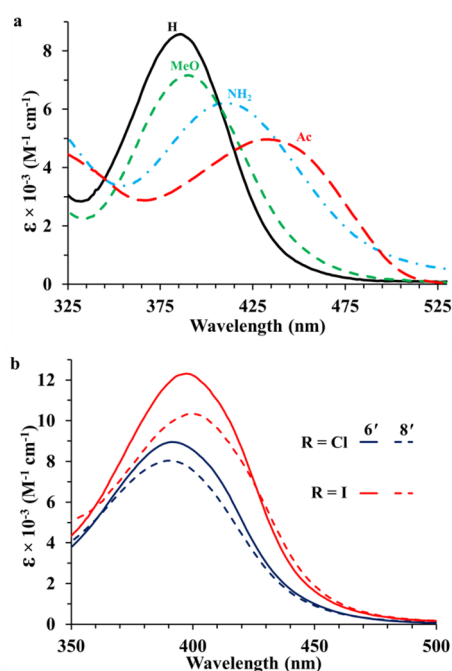


Figure 3. (a) UV-vis spectra of 8' DHI-7, -8, -13, (dashed) and H-DHI (solid curve) in dichloromethane. The introduction of amino, methoxy, or acetyl auxochromes red shifts the spiro λ_{\max} when compared to that of H-DHI. (b) UV-vis spectra of spiro 6' (solid curve) and 8' (dashed curves) isomers of DHI-10 and -11 in dichloromethane.

has a substantial red shift ($\lambda_{\max} = 440$) because of the long, extended π system. This is in contrast with the 6' and 7' systems, which are cross-conjugated and display dramatically smaller red shifts ($\lambda_{\max} = 426$ and 398 nm, respectively) from the unsubstituted species (H-DHI).

Although extended and cross-conjugation adequately explain the observed spectra, there are two nuances that must be mentioned. First, we cannot discount potential contributions of π -stacking interactions with the conjugated fluorene moiety. These interactions are ascribed to coplanar π systems with interplanar distances on the order of 3.3–3.8 Å.³⁶ As the distance between the fluorene and the substituent was calculated to be 3.3 Å for the 8' species (Supporting Information, Figure S5), such interactions are likely. Additional evidence of π -stacking interactions can be garnered from the ¹H NMR spectra of DHI-13, where the deshielding cone of the fluorene moiety substantially shifts the acetyl protons from 2.24 to 1.47 ppm for the 8' species.^{37,38} Second, although we do not wish to engage in substantial discussion of the relative absorbance of the chromophores (and the nuances of transition

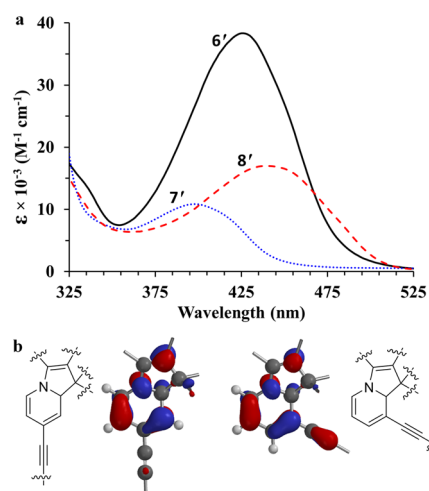


Figure 4. (a) UV-vis spectra of spiro 6', 7',²⁷ and 8' OPE-substituted DHI in dichloromethane. The two cross conjugated systems (6' and 7' isomers) display smaller red shifts than the extended conjugation of the 8' isomer. (b) Density functional theory calculations were used to generate the molecular orbitals of 7' and 8' alkynyl-substituted dihydropyridines. For the 7' isomer, the contribution to the HOMO from the alkynyl substituent is negligible, and the compound's optical properties are similar to those of an unsubstituted DHI. For the 8' system, there is continuous conjugation from the diene to the OPE system. The fluorene, OPE, and dimethyl maleate contribute minimally and are not shown in the interest of clarity. Full diagrams can be found in the Supporting Information (Figure S5).

dipoles), the significant increase in absorption for the 6' conformer is noteworthy. This effect is seen both in the acetyl- and OPE-substituted systems, with the extinction coefficient increasing roughly two to three times over the analogous 7' or 8' species. These effects have been seen before in cross-conjugated systems, although these are quite large in magnitude.³⁹

Zwitterion Stability. To examine the effect of the substituents on the zwitterion stability and the rate of cyclization back to the spiro species, the spiro DHIs were irradiated with 405 nm light (42 mW/cm²), which generated the zwitterion. The zwitterion maxima for all DHIs fall well within the accepted range (500–700 nm) of the presumed charge transfer band²² and are the same for both of the isolated conformers (Table 2). For the electrocyclization back to the spiro conformer, the decay of the zwitterion was measured as a function of time and, as predicted,²² followed a first-order rate.

The substituents have a substantial effect on the half-life of the zwitterionic species (Table 2). As the electron-donating ability of the substituent on the dihydropyridine increased, the

half-life also increased. This effect has been demonstrated by a linear relationship of DHIs half-lives with their appropriate Hammett parameters and was previously noted^{22,24} with asymmetric cyano DHIs. Any explanation for such results should center on the influence of the substituents on the isomerization process (*trans* to *cis*), which is the rate-determining step in the relaxation.²⁵

Two possible explanations suggest themselves. The first is the weakening of the double-bond character and stabilization of the transition state, which becomes more pronounced when both electron-withdrawing and -donating substituents are found, leading to a polarized ethylene and substantially lower barrier to rotation. This explanation is common in thermal isomerization literature.^{40,41} A second explanation is that the destabilization of the zwitterion accelerates the transition. We find the former mechanism to be less applicable (although not necessarily negligible), as such stabilization generally requires the ability to delocalize the double bond to the withdrawing substituent (in our case the pyridinium), which is less favorable for our system.^{21,22,24} Rather, the primary source is likely the stabilization/destabilization of the pyridinium via substituent effects. This is the more commonly accepted mechanism for the similar cyclization events.^{21,42,43}

Molecular Switch Design for Conformers. The above results allow one to create predictive rules for generating other similar photochromophores. To begin, cyclization occurring via the condensation reaction (Scheme 1) and resulting from the relaxation of the photoisomerized betaine produces the same ratio of constitutional isomers. Thus, compounds generated as a mixture of isomers are advantageous (providing access to both 6' and 8') despite the difficulties associated with their separation, especially in the case of DHI-9. The data here shows that for a wide range of substituents, the dimethyl maleate system seems ideal for generating this mixture, occurring for all but the extremely donating amino group. This ability to generate both conformers is impressive considering that the only prior attempt to do so generated exclusively the 8' for the majority of substituents (including chloro, methyl, and methoxy).²¹ The difference, in our case, stems from the methyl esters on the dihydropyrrole, which are cyano groups for previous reports. In essence, the dihydropyrrole substituent causes a substantial shift in thermodynamic stability of the 6' isomer relative to that of the 8', but fine-tuning of the isomer composition is dictated by the substituents on the pyridine ring.

These pyridial substituents play a role in the optical properties of the DHIs, just as they impact the isomer composition of the spiro species. Again, from a design standpoint, it would be ideal if the change in λ_{\max} could be controlled via a parameter that is not correlated with electron donation/withdrawal, as this tunes isomer composition, and thus the optical properties could be controlled independently. Conveniently, the two are quite uncorrelated, and instead, control over the absorption properties is governed by the Woodward–Fieser rules. Figure 5 demonstrates both the decoupling of the λ_{\max} from the isomeric ratio and the predictive ability of the Woodward–Fieser rules. For the former, the shift in λ_{\max} is plotted against σ_R and σ_I (used as a surrogate for thermodynamic stability) and shows no correlation. For the latter, both the expected and measured shifts match exquisitely in instances where both are available (red diamonds vs black squares, e.g. –OMe). Despite the successes of these models on simple substituents, conjugated

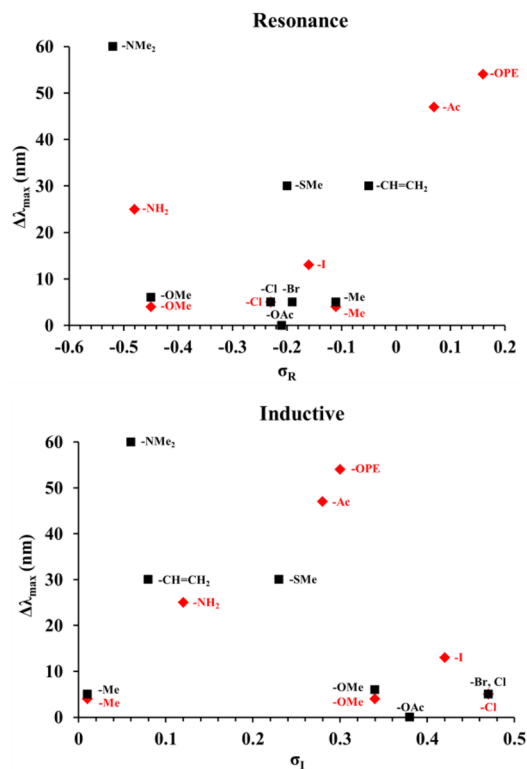


Figure 5. Shift in λ_{\max} , both measured and predicted, for DHIs. Common data points for the measured (red diamonds) and of empirical Woodward–Fieser³¹ (black squares) substituents for butadiene systems are virtually identical, showing a strong predictive ability of the Woodward–Fieser rules. When both sets of data for $\Delta\lambda_{\max}$ are plotted against their respective resonance (top) and inductive (bottom) Hammett parameters,⁴⁴ no correlation is seen, indicating that these parameters can be tuned independently. In the case of the OPE and Ac substituents, the reported λ_{\max} is for the 8' isomer, as the effect of cross-conjugation is minimal for these species.

substituents at the 6' or 7' position are governed by cross-conjugation and should be considered separately. For all of the systems studied though, the isomer ratio can be controlled independently from the absorbance maximum.

The final parameter is half-life, and here we find that the property is correlated to the isomer ratio but not to the excitation wavelength. The relationship between the isomer composition and half-life should not surprise, as both have been correlated to electron-donation ability/Hammett parameters, and we have already described how λ_{\max} is relatively independent of these parameters. The correlation between isomer composition and half-life, however, provides the one limitation on the design of similar DHI photochromophores: both a long half-life and generation of the 6' conformer appear mutually exclusive. It remains to be seen if other substitutions (e.g., a dihydropyridazine- or dihydroisoquinoline-based system) allow circumvention of this issue.

CONCLUSIONS

We synthesized a series of asymmetric DHIs containing both electron-donating and -withdrawing substituents on the dihydropyridine ring in order to investigate the substituents influence over isomer control and their intertwined effects on the optical properties and the molecular switch's half-life. As electron donors are introduced to the dihydropyridine, the effect was 2-fold: the population of the 8' isomer was favored

and the generated DHIs displayed an enhanced stability in the zwitterion form. With electron-withdrawing groups, the electrocyclicization rate was enhanced along with the increased formation of the 6' isomer. In contrast, the optical absorption for the system could be tuned with relative independence of the isomer ratio and half-life; this parameter is primarily governed (empirically) by the Woodward–Fieser rules. Overall, both the 6' and 8' isomers were accessible for all substituents save one. These form the basis for the design parameters to be used in building more complex photoswitches for smart electronics.

EXPERIMENTAL SECTION

General Experimental Methods. NMR spectra were taken on a 500 MHz spectrometer. ¹H chemical shifts (δ) for spectra acquired in CDCl₃ were referenced to tetramethylsilane (0 ppm). 8'-DHI-7 was taken in, and referenced to, CD₂Cl₂ at 5.32 ppm, and DHI-10s, DHI-11s, DHI-12s, and 6'-DHI-13 were taken in, and referenced to, CD₃CN at 1.94 ppm. All ¹³C spectra were referenced to CDCl₃ at 77.23 ppm. Reactions were run under a nitrogen atmosphere unless otherwise noted. All plug purifications and column chromatography separations were carried out on silica gel 60 (40–63 μ m from BDH). Thin-layer chromatography (TLC) was performed on silica gel 60 (F₂₅₄) with glass support. Dimethyl spiro[cycloprop[2]ene-1,9'-fluorene]-2,3-dicarboxylate,²⁷ 3-methoxy-pyridine,⁴⁵ Pd(PPh₃)₂Cl₂,⁴⁶ H-DHI,¹⁷ and DHI-1²⁷ were made according to previously reported procedures. High-resolution mass spectra samples were ionized by ion trap (IT) or electrospray ionization (ESI) and recorded via the time-of-flight (TOF) method. Dichloromethane was used as the solvent for all UV–vis spectra measurements, and IR spectra of either liquid films or KBr samples were acquired on a FT-IR with a liquid nitrogen-cooled MCT detector. Calculations of the two valence occupied molecular orbitals in Figure 4b were performed with Spartan '08 using the B3LYP/6-31G* density functional theory method. The zwitterion λ_{max} for DHI-12 and -13 were obtained by means of a Gaussian fit.

General Condensation Procedure. For the condensations, dimethyl spiro[cycloprop[2]ene-1,9'-fluorene]-2,3-dicarboxylate was mixed with the respective pyridial derivative in a 1:1 mole ratio. The round-bottomed flask was purged with nitrogen for 30 min in the dark at room temperature before the addition of chloroform, THF, or dichloromethane. Reaction mixtures were allowed to stir for 2–24 h, and the solvent was removed by rotary evaporation. All reactions were purified via column chromatography except for 8'-DHI-7, which proved to be metastable.

Dimethyl 8'-Amino-8a'H-spiro[fluorene-9,1'-indolizine]-2',3'-dicarboxylate (8'-DHI-7). Dimethyl spiro[cycloprop[2]ene-1,9'-fluorene]-2,3-dicarboxylate (0.043 g, 0.14 mmol), 3-aminopyridine (0.13 g, 0.14 mmol), and CH₂Cl₂ (5 mL) were added to a round-bottomed flask according to the general DHI procedure and stirred for 5 h. 8'-DHI-7 (0.050 g, 0.12 mmol) was generated in 86% yield as an orange oil. ¹H NMR (500 MHz, CD₂Cl₂) δ 7.78–7.75 (m, 2H), 7.66 (d, *J* = 7.6 Hz, 1H), 7.52 (d, *J* = 7.6 Hz, 1H), 7.46–7.37 (m, 3H), 7.27 (dt, *J* = 7.4, 1.1 Hz, 1H), 6.09 (d, *J* = 7.5 Hz, 1H), 5.58 (s, 1H), 5.23 (t, *J* = 6.8 Hz, 1H), 4.73 (dd, *J* = 6.4, 2.0 Hz, 1H), 3.95 (s, 3H), 3.27 (s, 3H), 2.33 (s, 2H). ¹³C NMR (125 MHz, CDCl₃) δ 164.0, 162.7, 148.3, 147.7, 143.9, 141.3, 139.8, 136.9, 128.9, 128.5, 128.1, 127.9, 124.2, 124.1, 120.4, 120.3, 115.6, 107.1, 107.0, 95.1, 70.2, 64.2, 53.4, 51.0. IR (liquid film, cm⁻¹): 3361, 2952, 1742, 1691, 1642, 1575, 1438, 1390, 1348, 1301, 1242, 1191, 1147, 1127, 1105. HRMS (IT-TOF) calcd for C₂₄H₁₉N₂O₄[M - H]⁻, 399.1350; found, 399.1361.

DHI-8s. Dimethyl spiro[cycloprop[2]ene-1,9'-fluorene]-2,3-dicarboxylate (0.254 g, 0.83 mmol), 3-methoxy-pyridine (0.091 g, 0.83 mmol), and CHCl₃ (40 mL) were added to a round-bottomed flask according to the general DHI procedure and stirred for 5 h. The product, 8'-DHI-8 (0.285 g, 0.69 mmol), was isolated via column chromatography (100% CH₂Cl₂, *R*_f = 0.53) in 83% yield as a yellow oil.

6'-Isomer: Dimethyl 6'-Methoxy-8a'H-spiro[fluorene-9,1'-indolizine]-2',3'-dicarboxylate (6'-DHI-8). Indicative 6'-isomer

peaks allowing for quantification assigned from crude mixture; ¹H NMR (500 MHz, CDCl₃) δ 5.93 (s, 1H), 5.69–5.65 (m, 1H), 5.38–5.36 (m, 1H), 4.66–4.63 (m, 1H), 4.01 (s, 3H), 3.56 (s, 3H).

8'-Isomer: Dimethyl 8'-Methoxy-8a'H-spiro[fluorene-9,1'-indolizine]-2',3'-dicarboxylate (8'-DHI-8). (100% CH₂Cl₂, *R*_f = 0.53). ¹H NMR (500 MHz, CDCl₃) δ 7.72–7.69 (m, 2H), 7.55 (d, *J* = 7.3 Hz, 1H), 7.44 (d, *J* = 7.3 Hz, 1H), 7.36 (dt, *J* = 7.4, 1.1 Hz, 1H), 7.34–7.29 (m, 2H), 7.18 (dt, *J* = 7.4, 1.0 Hz, 1H), 6.14 (d, *J* = 7.3 Hz, 1H), 5.58–5.57 (m, 1H), 5.20 (t, *J* = 6.8 Hz, 1H), 4.77 (dd, *J* = 6.6, 2.0 Hz, 1H), 3.98 (s, 3H), 3.25 (s, 3H), 2.75 (s, 3H). ¹³C NMR (125 MHz, CDCl₃) δ 164.1, 162.6, 150.6, 149.0, 147.8, 144.2, 142.1, 140.8, 128.1, 127.7, 127.4, 126.8, 123.2, 123.1, 119.8, 119.7, 117.7, 108.6, 104.9, 93.6, 70.0, 64.8, 54.5, 53.4, 51.1. IR (liquid film, cm⁻¹): 3015, 2952, 2929, 2852, 1745, 1706, 1692, 1643, 1579, 1448, 1438, 1425, 1392, 1379, 1346, 1296, 1262, 1240, 1225, 1190, 1146, 1126, 1105, 1036. HRMS (ESI-TOF) calcd for C₂₅H₂₁NO₅H⁺ [M + H]⁺, 416.1492; found, 416.1506.

DHI-9s. Dimethyl spiro[cycloprop[2]ene-1,9'-fluorene]-2,3-dicarboxylate (0.043 g, 0.14 mmol), 3-picoline (0.013 g, 0.14 mmol), and CH₂Cl₂ (10 mL) were added to a round-bottomed flask according to the general DHI procedure and stirred for 4 h. The product, 8'-DHI-9 (0.034 g, 0.085 mmol), was isolated via column chromatography (100% CH₂Cl₂, *R*_f = 0.17) in 61% yield of as a yellow oil.

Selective Indicative ¹H NMR (500 MHz, CDCl₃) Peaks for 6'-Isomer: Dimethyl 6'-Methyl-8a'H-spiro[fluorene-9,1'-indolizine]-2',3'-dicarboxylate (6'-DHI-9). δ 6.21–6.19 (m, 1H), 5.40–5.38 (m, 1H), 4.52 (d, *J* = 10.0 Hz, 1H), 4.01 (s, 3H), 3.26 (s, 3H), 1.73 (s, 3H).

8'-Isomer: Dimethyl 8'-Methyl-8a'H-spiro[fluorene-9,1'-indolizine]-2',3'-dicarboxylate (8'-DHI-9). (100% CH₂Cl₂, *R*_f = 0.17) ¹H NMR (500 MHz, CDCl₃) δ 7.71 (d, *J* = 7.3 Hz, 2H), 7.57 (d, *J* = 7.3 Hz, 1H), 7.54 (d, *J* = 7.6 Hz, 1H), 7.40–7.36 (m, 2H), 7.32 (dt, *J* = 7.3, 1.2 Hz, 1H), 7.23 (dt, *J* = 7.5, 1.1 Hz, 1H), 6.32 (d, *J* = 7.6 Hz, 1H), 5.58 (s, 1H), 5.45–5.41 (m, 1H), 5.14 (dd, *J* = 7.4, 6.0 Hz, 1H), 3.98 (s, 3H), 3.24 (s, 3H), 0.63 (s, 3H). ¹³C NMR (125 MHz, CDCl₃) δ 164.1, 162.7, 148.5, 146.9, 144.2, 142.1, 140.6, 128.65, 128.60, 128.1, 127.6, 127.5, 124.2, 123.7, 122.7, 120.5, 120.2, 120.1, 108.9, 104.6, 72.7, 64.8, 53.4, 51.1, 17.7. IR (liquid film, cm⁻¹): 2951, 2924, 2852, 1744, 1704, 1645, 1599, 1571, 1448, 1428, 1391, 1344, 1301, 1260, 1239, 1226, 1191, 1146, 1125, 1106, 1066. HRMS (IT-TOF) calcd for C₂₅H₂₁NO₄H⁺ [M + H]⁺, 400.1543; found, 400.1548.

DHI-10s. Dimethyl spiro[cycloprop[2]ene-1,9'-fluorene]-2,3-dicarboxylate (0.064 g, 0.21 mmol), 3-iodopyridine (0.043 g, 0.21 mmol), and CH₂Cl₂ (10.5 mL) were added to a round-bottomed flask according to the general DHI procedure and stirred for 14 h. The 8'-isomer was isolated via column chromatography (3:1 hexanes/EtOAc). The 6' isomer was then separated from the reagents and side products via a second column (100% CH₂Cl₂). DHI-10 (0.070 g, 0.14 mmol) was obtained in 67% combined yield as a yellow oil.

6'-Isomer: Dimethyl 6'-Iodo-8a'H-spiro[fluorene-9,1'-indolizine]-2',3'-dicarboxylate (6'-DHI-10). (0.008 g, 100% CH₂Cl₂, *R*_f = 0.63). ¹H NMR (500 MHz, CD₃CN) δ 7.82–7.78 (m, 2H), 7.59 (d, *J* = 7.3 Hz, 1H), 7.44–7.40 (m, 3H), 7.35 (dt, *J* = 7.5, 1.1 Hz, 1H), 7.30–7.27 (m, 1H), 6.94–6.93 (m, 1H), 5.66 (ddd, *J* = 10.0, 2.6, 1.0 Hz, 1H), 5.54–5.52 (m, 1H), 4.28 (ddd, *J* = 10.1, 2.0, 1.0 Hz, 1H), 3.96 (s, 3H), 3.28 (s, 3H). ¹³C NMR (125 MHz, CDCl₃) δ 163.7, 161.9, 146.9, 145.6, 141.91, 141.87, 140.6, 131.1, 130.0, 128.8, 128.5, 128.0, 127.4, 124.9, 123.7, 120.3, 120.0, 119.0, 109.8, 68.2, 65.1, 64.3, 53.6, 51.3. IR (liquid film, cm⁻¹): 2951, 2925, 2854, 1743, 1703, 1596, 1546, 1438, 1416, 1369, 1324, 1306, 1262, 1229, 1189, 1166, 1131, 1107, 1074, 1047. HRMS (IT-TOF) calcd for C₂₄H₁₈INO₄H⁺ [M + H]⁺, 512.0353; found, 512.0364.

8'-Isomer: Dimethyl 8'-Iodo-8a'H-spiro[fluorene-9,1'-indolizine]-2',3'-dicarboxylate (8'-DHI-10). (0.062 g, 3:1 hexanes/EtOAc, *R*_f = 0.68). ¹H NMR (500 MHz, CD₃CN) δ 7.79–7.75 (m, 2H), 7.58 (d, *J* = 7.6 Hz, 1H), 7.49 (d, *J* = 7.6 Hz, 1H), 7.46–7.41 (m, 2H), 7.36 (dt, *J* = 7.5, 1.1 Hz, 1H), 7.29 (dt, *J* = 7.4, 1.0 Hz, 1H), 6.62 (d, *J* = 7.3 Hz, 1H), 6.48 (dd, *J* = 6.2, 2.3 Hz, 1H), 5.89 (d, *J* = 2.5 Hz, 1H), 4.97–4.94 (m, 1H), 3.93 (s, 3H), 3.25 (s, 3H). ¹³C NMR (125 MHz, CDCl₃) δ 163.6, 162.1, 147.5, 145.9, 143.6, 142.5, 142.2, 136.0,

128.9, 128.4, 127.6, 127.4, 125.4, 124.4, 123.7, 120.20, 120.16, 111.5, 103.7, 83.7, 72.3, 66.4, 53.5, 51.3. IR (liquid film, cm^{-1}): 2952, 2925, 2854, 1743, 1710, 1598, 1543, 1448, 1436, 1427, 1384, 1356, 1295, 1254, 1227, 1191, 1147, 1125, 1106. HRMS (IT-TOF) calcd for $\text{C}_{24}\text{H}_{18}\text{INO}_4\text{H}^+ [\text{M} + \text{H}]^+$, 512.0353; found, 512.0338.

DHI-11s. Dimethyl spiro[cycloprop[2]ene-1,9'-fluorene]-2,3-dicarboxylate (0.150 g, 0.49 mmol), 3-chloropyridine (0.056 g, 0.49 mmol), and CHCl_3 (22 mL) were added to a round-bottomed flask according to the general DHI procedure and stirred for 9 h. The crude mixture was first passed through a silica plug (CH_2Cl_2), and then the two eluted isomers were separated via column chromatography (3:1 hexanes/EtOAc) to afford **DHI-11s** (0.116 g, 0.28 mmol) in 57% combined yield as a yellow oil.

6'-Isomer: Dimethyl 6'-Chloro-8a'H-spiro[fluorene-9,1'-indolizine]-2',3'-dicarboxylate (6'-DHI-11). (0.026 g, $R_f = 0.40$). ^1H NMR (500 MHz, CD_3CN) δ 7.82–7.79 (m, 2H), 7.60 (d, $J = 7.6$ Hz, 1H), 7.44–7.40 (m, 3H), 7.36 (t, $J = 7.4$ Hz, 1H), 7.28 (t, $J = 7.4$ Hz, 1H), 6.76 (s, 1H), 5.69 (d, $J = 10.0$ Hz, 1H), 5.52–5.50 (m, 1H), 4.43 (d, $J = 10.3$ Hz, 1H), 3.96 (s, 3H), 3.28 (s, 3H). ^{13}C NMR (125 MHz, CDCl_3) δ 163.7, 161.9, 147.0, 146.2, 142.0, 141.9, 140.6, 128.8, 128.5, 128.0, 127.4, 126.2, 124.8, 123.7, 122.3, 120.3, 120.0, 118.9, 112.2, 109.7, 69.1, 64.2, 53.6, 51.3. IR (liquid film, cm^{-1}): 2952, 2925, 2854, 1743, 1705, 1596, 1558, 1439, 1421, 1392, 1369, 1324, 1303, 1262, 1228, 1131, 1108, 1069. HRMS (IT-TOF) calcd for $\text{C}_{24}\text{H}_{18}\text{ClNO}_4\text{H}^+ [\text{M} + \text{H}]^+$, 420.0997; found, 420.1007.

8'-Isomer: Dimethyl 8'-Chloro-8a'H-spiro[fluorene-9,1'-indolizine]-2',3'-dicarboxylate (8'-DHI-11). (0.090 g, $R_f = 0.22$). ^1H NMR (500 MHz, CD_3CN) δ 7.79–7.76 (m, 2H), 7.60 (d, $J = 7.3$ Hz, 1H), 7.48 (d, $J = 7.3$ Hz, 1H), 7.44–7.39 (m, 2H), 7.35 (dt, $J = 7.4, 1.1$ Hz, 1H), 7.28 (dt, $J = 7.4, 1.0$ Hz, 1H), 6.55 (d, $J = 7.3$ Hz, 1H), 5.90–5.84 (m, 2H), 5.17 (t, $J = 7.0$ Hz, 1H), 3.94 (s, 3H), 3.26 (s, 3H). ^{13}C NMR (125 MHz, CDCl_3) δ 163.7, 162.1, 147.7, 146.2, 142.9, 142.5, 141.4, 128.8, 128.2, 127.5, 127.3, 124.1, 123.8, 123.4, 123.2, 123.1, 120.2, 120.1, 111.1, 102.5, 71.7, 65.5, 53.5, 51.3. IR (liquid film, cm^{-1}): 2953, 2925, 2854, 1744, 1711, 1637, 1600, 1560, 1448, 1437, 1361, 1340, 1294, 1256, 1227, 1192, 1148, 1127, 1107, 1086. HRMS (IT-TOF) calcd for $\text{C}_{24}\text{H}_{18}\text{ClNO}_4\text{H}^+ [\text{M} + \text{H}]^+$, 420.0997; found, 420.0979.

DHI-12s. Dimethyl spiro[cycloprop[2]ene-1,9'-fluorene]-2,3-dicarboxylate (0.038 g, 0.12 mmol), (4-thioacetylphenyl)(3-pyridyl)acetylene (0.030 g, 0.12 mmol), and THF (8 mL) were added to a round-bottomed flask according to the general DHI procedure and stirred for 15 h. The two isomers were isolated via column chromatography (2:1 hexanes/EtOAc) to afford **DHI-12** (0.062 g, 0.11 mmol) in 92% combined yield as a yellow oil.

6'-Isomer: Dimethyl 6'-((4-(Acetylthio)phenyl)ethynyl)-8a'H-spiro[fluorene-9,1'-indolizine]-2',3'-dicarboxylate (6'-DHI-12). (0.034 g, $R_f = 0.53$). ^1H NMR (500 MHz, CD_3CN) δ 7.84–7.81 (m, 2H), 7.62 (d, $J = 7.8$ Hz, 1H), 7.46–7.41 (m, 5H), 7.39–7.35 (m, 3H), 7.30 (dt, $J = 7.6, 1.0$ Hz, 1H), 7.05 (d, $J = 1.0$ Hz, 1H), 5.78 (ddd, $J = 10.0, 2.6, 1.0$ Hz, 1H), 5.58–5.56 (m, 1H), 4.45–4.42 (m, 1H), 3.99 (s, 3H), 3.31 (s, 3H), 2.39 (s, 3H). ^{13}C NMR (125 MHz, CDCl_3) δ 193.7, 163.6, 161.8, 146.6, 145.6, 141.9, 141.8, 140.6, 134.4, 131.8, 130.0, 128.8, 128.5, 128.0, 127.5, 127.4, 125.6, 125.0, 124.8, 123.7, 120.4, 120.1, 117.0, 112.2, 99.8, 89.8, 88.8, 69.1, 64.4, 53.7, 51.4, 30.4. IR (liquid film, cm^{-1}): 2952, 2924, 2853, 1742, 1707, 1632, 1559, 1551, 1488, 1438, 1421, 1373, 1309, 1264, 1226, 1191, 1121, 1105. HRMS (ESI-TOF) calcd for $\text{C}_{34}\text{H}_{25}\text{NO}_5\text{S} [\text{M} + \text{H}]^+$, 560.1526; found, 560.1534.

8'-Isomer: Dimethyl 8'-((4-(Acetylthio)phenyl)ethynyl)-8a'H-spiro[fluorene-9,1'-indolizine]-2',3'-dicarboxylate (8'-DHI-12). (0.028 g, $R_f = 0.40$). ^1H NMR (500 MHz, CD_3CN) δ 7.76 (d, $J = 7.1$ Hz, 1H), 7.69 (d, $J = 7.3$ Hz, 1H), 7.64 (d, $J = 7.1$ Hz, 1H), 7.49 (d, $J = 7.6$ Hz, 1H), 7.40 (dt, $J = 7.4, 1.1$ Hz, 1H), 7.36 (dt, $J = 7.5, 1.2$ Hz, 1H), 7.32 (dt, $J = 7.4, 1.1$ Hz, 1H), 7.27–7.24 (m, 3H), 6.83 (dd, $J = 6.5, 1.8$ Hz, 2H), 6.70 (d, $J = 7.3$ Hz, 1H), 6.19 (dd, $J = 6.1, 2.2$ Hz, 1H), 5.77–5.74 (m, 1H), 5.34 (dd, $J = 7.3, 6.3$ Hz, 1H), 3.96 (s, 3H), 3.26 (s, 3H), 2.39 (s, 3H). ^{13}C NMR (125 MHz, CDCl_3) δ 193.7, 163.7, 162.2, 147.7, 145.8, 142.84, 142.77, 141.7, 133.7, 132.0, 131.3, 128.6, 128.1, 127.57, 127.55, 127.3, 126.3, 124.2, 124.1, 123.6,

120.2, 120.1, 111.8, 110.9, 104.1, 92.7, 87.9, 69.1, 64.7, 53.5, 51.3, 30.4. IR (liquid film, cm^{-1}): 2952, 2925, 2854, 1744, 1708, 1595, 1529, 1487, 1450, 1432, 1408, 1352, 1301, 1256, 1228, 1191, 1150, 1124, 1091, 1016. HRMS (ESI-TOF) calcd for $\text{C}_{34}\text{H}_{25}\text{NO}_5\text{SH}^+ [\text{M} + \text{H}]^+$, 560.1526; found, 560.1531.

DHI-13s. Dimethyl spiro[cycloprop[2]ene-1,9'-fluorene]-2,3-dicarboxylate (0.058 g, 0.19 mmol), 3-acetylpyridine (0.023 g, 0.19 mmol), and CHCl_3 (9.5 mL) were added to a round-bottomed flask according to the general DHI procedure and stirred for 2 h. The product was isolated via column chromatography (1:1 hexanes/EtOAc) to afford the two isomers of **DHI-13** (0.064 g, 0.15 mmol) in 79% combined yield as a yellow oil.

6'-Isomer: Dimethyl 6'-Acetyl-8a'H-spiro[fluorene-9,1'-indolizine]-2',3'-dicarboxylate (6'-DHI-13). (0.039 g, $R_f = 0.50$). ^1H NMR (500 MHz, CD_3CN) δ 7.84–7.81 (m, 2H), 7.61 (d, $J = 7.6$ Hz, 1H), 7.57 (s, 1H), 7.47–7.41 (m, 2H), 7.40–7.35 (m, 2H), 7.28 (t, $J = 7.6$ Hz, 1H), 6.26 (dd, $J = 10.3, 2.4$ Hz, 1H), 5.61–5.59 (m, 1H), 4.35 (d, $J = 10.0$ Hz, 1H), 4.00 (s, 3H), 3.34 (s, 3H), 2.20 (s, 3H). ^{13}C NMR (125 MHz, CDCl_3) δ 193.0, 163.2, 161.3, 145.8, 144.4, 142.0, 141.2, 140.6, 134.4, 129.0, 128.8, 128.0, 127.5, 124.7, 123.6, 122.1, 120.5, 120.2, 117.7, 116.9, 115.2, 69.6, 64.6, 53.8, 51.7, 25.2. IR (liquid film, cm^{-1}): 2953, 2927, 1741, 1731, 1650, 1630, 1611, 1556, 1535, 1438, 1376, 1315, 1287, 1259, 1212, 1184, 1132, 1109, 1066, 1037. HRMS (ESI-TOF) calcd for $\text{C}_{26}\text{H}_{21}\text{NO}_5\text{H}^+ [\text{M} + \text{H}]^+$, 428.1492; found, 428.1504.

8'-Isomer: Dimethyl 8'-Acetyl-8a'H-spiro[fluorene-9,1'-indolizine]-2',3'-dicarboxylate (8'-DHI-13). (0.025 g, $R_f = 0.55$). ^1H NMR (500 MHz, CDCl_3) δ 7.70 (d, $J = 7.6$ Hz, 1H), 7.67 (d, $J = 7.6$ Hz, 1H), 7.55 (d, $J = 7.1$ Hz, 1H), 7.50 (d, $J = 7.3$ Hz, 1H), 7.40 (dt, $J = 7.3, 1.2$ Hz, 1H), 7.37–7.30 (m, 2H), 7.16 (dt, $J = 7.3, 1.0$ Hz, 1H), 6.68 (d, $J = 7.3$ Hz, 1H), 6.52–6.50 (m, 1H), 6.01–5.99 (m, 1H), 5.28–5.24 (m, 1H), 3.97 (s, 3H), 3.24 (s, 3H), 1.48 (s, 3H). ^{13}C NMR (125 MHz, CDCl_3) δ 194.1, 163.6, 162.0, 148.7, 145.1, 142.1, 142.0, 141.7, 131.7, 131.2, 129.4, 128.5, 127.7, 127.5, 126.3, 124.1, 122.3, 120.5, 119.7, 113.9, 101.9, 69.4, 65.9, 53.5, 51.4, 24.5. IR (liquid film, cm^{-1}): 2953, 2925, 2853, 1743, 1714, 1665, 1610, 1535, 1449, 1439, 1383, 1354, 1295, 1271, 1227, 1149, 1127, 1105, 1042, 1004. HRMS (ESI-TOF) calcd for $\text{C}_{26}\text{H}_{21}\text{NO}_5\text{H}^+ [\text{M} + \text{H}]^+$, 428.1492; found, 428.1499.

3-Iodopyridine. To a round-bottomed flask open to the atmosphere, paratoulene sulfonic acid (9.393 g, 49.38 mmol) was mixed with acetonitrile (60 mL) and was added to 3-aminopyridine (1.500 g, 16.46 mmol). The mixture was cooled to 10 °C, and an aqueous solution (10 mL) containing NaNO_2 (2.27 g, 32.92 mmol) and KI (6.831 g, 40.15 mmol) was added dropwise. The slurry was stirred for 10 min at 10 °C and then brought to room temperature for 1 h. The reaction was brought to a pH 9–10 via 1 M NaHCO_3 (aq) and then decolorized from a dark brown to a light orange with 2 M $\text{Na}_2\text{S}_2\text{O}_3$ (aq). The reaction was then diluted and extracted ($\times 3$) with ethyl acetate. The combined organic layers were dried with MgSO_4 and filtered, the solvent was removed via rotary evaporation, and column chromatography (2:1 hexanes/EtOAc, $R_f = 0.53$) was used to isolate 3-iodopyridine (1.675 g, 8.171 mmol) in 48% yield as an off white solid. mp 52–53 °C. ^1H NMR (500 MHz, CDCl_3) δ 8.85 (d, $J = 1.5$ Hz, 1H), 8.56 (dd, $J = 4.9, 1.5$ Hz, 1H), 8.03–8.00 (m, 1H), 7.12–7.09 (m, 1H).⁴⁷

3-(Trimethylsilylethynyl)pyridine. $\text{Pd}(\text{PPh}_3)_2\text{Cl}_2$ (0.086 g, 0.12 mmol), 3-iodopyridine (1.258 g, 6.137 mmol), and CuI (0.047 g, 0.25 mmol) were added to a sealed tube that was evacuated and filled with nitrogen five times. THF (12 mL), triethylamine (1.7 mL), and TMSA (0.96 mL) were added via a syringe while stirring, and the brown mixture was stirred for 12 h at 40 °C. The crude mixture was poured into water, extracted with CH_2Cl_2 ($\times 3$), dried with MgSO_4 , and filtered. The solvent was removed via rotary evaporation, and the product was isolated by column chromatography (3:1 hexanes/EtOAc, $R_f = 0.45$), which afforded 3-(trimethylsilylethynyl)pyridine (0.872 g, 4.97 mmol) as a dark oil in 81% yield. ^1H NMR (500 MHz, CDCl_3) δ 8.69 (d, $J = 1.5$ Hz, 1H), 8.53 (dd, $J = 4.9, 1.7$ Hz, 1H), 7.74 (dt, $J = 7.8, 1.9$ Hz, 1H), 7.25–7.21 (m, 1H), 0.27 (s, 9H).⁴⁸

3-Ethynylpyridine. 3-(Trimethylsilylethynyl)pyridine (1.000 g, 5.701 mmol) was dissolved in MeOH (9 mL) and CH₂Cl₂ (18 mL) in a round-bottomed flask. Anhydrous KOH (0.640 g, 11.4 mmol) was added to the mixture, which was then stirred for 1.5 h. The reaction was partitioned between CH₂Cl₂ and water, and the aqueous layer was further extracted two times with CH₂Cl₂. The combined organic solution was then dried with MgSO₄, and the solvent was removed by rotary evaporation, which afforded 3-ethynylpyridine (0.581 g, 5.63 mmol) as an off-white solid in 99% yield. ¹H NMR (500 MHz, (CD₃)₂CO) δ 8.68 (d, J = 1.2 Hz, 1H), 8.58 (dd, J = 4.8, 1.3 Hz, 1H), 7.87 (dt, J = 7.8, 2.0 Hz, 1H), 7.42–7.38 (m, 1H), 3.88 (s, 1H).⁴⁹

(4-Thioacetylphenyl)(3-pyridyl)acetylene. Pd(PPh₃)₂Cl₂ (0.013 g, 0.018 mmol), 4-iodophenyl thioacetate (0.167 g, 0.600 mmol), 3-ethynylpyridine (0.068 g, 0.66 mmol), and CuI (0.007 g, 0.036 mmol) were added to a sealed tube that was evacuated and filled with nitrogen five times. THF (15 mL) and triethylamine (0.48 mL, 3.4 mmol) were added via a syringe while stirring, and the dark brown mixture was stirred for 18.5 h at 40 °C. The crude mixture was poured into water, extracted with CH₂Cl₂ (×3), dried with MgSO₄, and filtered. Solvent was removed via rotary evaporation, and the product was isolated by column chromatography (1:2 hexanes/EtOAc, R_f = 0.56), which afforded (4-thioacetylphenyl)(3-pyridyl)acetylene (0.030 g, 0.12 mmol) as an off white solid in 70% yield from recovered starting material. mp 95–98 °C. ¹H NMR (500 MHz, CDCl₃) δ 8.77 (d, J = 2.0 Hz, 1H), 8.57 (dd, J = 4.9, 1.5 Hz, 1H), 7.82, (dt, J = 7.8, 2.0 Hz, 1H), 7.57 (dd, J = 6.5, 1.8 Hz, 2H), 7.42 (dd, J = 6.5, 1.8 Hz, 2H), 7.30 (d, J = 7.8 Hz, 1H), 2.45 (s, 3H). ¹³C NMR (125 MHz, CDCl₃) δ 193.4, 152.5, 149.1, 138.7, 134.5, 132.4, 129.0, 123.9, 123.3, 120.3, 92.0, 87.7, 30.5. IR (KBr, cm⁻¹): 1707, 1559, 1490, 1408, 1120, 1093, 1016. HRMS (ESI-TOF) calcd for C₁₅H₁₁NOSH⁺ [M + H]⁺, 254.0634; found, 254.0637.

■ ASSOCIATED CONTENT

■ Supporting Information

IR, ¹H NMR, and ¹³C NMR spectra of targeted DHIs and (4-thioacetylphenyl)(3-pyridyl)acetylene and UV–vis spectroscopy of spiro and zwitterion DHIs. This material is available free of charge via the Internet at <http://pubs.acs.org>.

■ AUTHOR INFORMATION

Corresponding Author

*E-mail: jciszek@luc.edu. Phone: (773) 508-3107.

Notes

The authors declare no competing financial interest.

■ ACKNOWLEDGMENTS

This work was supported in part by a grant from the National Science Foundation (NSF), Career Award no. 1056400.

■ REFERENCES

- Crivillers, N.; Orgiu, E.; Reinders, F.; Mayor, M.; Samori, P. *Adv. Mater.* **2011**, *23*, 1447.
- Ah Qune, L. F. N.; Akiyama, H.; Nagahiro, T.; Tamada, K.; Wee, A. T. S. *Appl. Phys. Lett.* **2008**, *93*, 083109.
- Suda, M.; Kameyama, N.; Ikegami, A.; Einaga, Y. *J. Am. Chem. Soc.* **2009**, *131*, 865.
- Nagahiro, T.; Akiyama, H.; Hara, M.; Tamada, K. *J. Electron Spectrosc. Relat. Phenom.* **2009**, *172*, 128.
- Bartucci, M. A.; Florián, J.; Ciszek, J. W. *J. Phys. Chem. C* **2013**, *117*, 19471.
- Campbell, I. H.; Kress, J. D.; Martin, R. L.; Smith, D. L.; Barashkov, N. N.; Ferraris, J. P. *Appl. Phys. Lett.* **1997**, *71*, 3528.
- Campbell, I. H.; Rubin, S.; Zawodzinski, T. A.; Kress, J. D.; Martin, R. L.; Smith, D. L.; Barashkov, N. N.; Ferraris, J. P. *Phys. Rev. B* **1996**, *54*, 14321.
- Ishii, H.; Sugiyama, K.; Ito, E.; Seki, K. *Adv. Mater.* **1999**, *11*, 605.

- Kelley, T. W.; Baude, P. F.; Gerlach, C.; Ender, D. E.; Muires, D.; Hasse, M. A.; Vogel, D. E.; Theiss, S. D. *Chem. Mater.* **2004**, *16*, 4413.
- Ratner, M. *Nature* **2000**, *404*, 137.
- Hamadani, B. H.; Corley, D. A.; Ciszek, J. W.; Tour, J. M.; Natelson, D. *Nano Lett.* **2006**, *6*, 1303.
- Howell, S.; Kuila, D.; Kasibhatla, B.; Kubiak, C. P.; Janes, D.; Reifenger, R. *Langmuir* **2002**, *18*, 5120.
- Comstock, M. J.; Levy, N.; Kirakosian, A.; Cho, J.; Lauterwasser, F.; Harvey, J. H.; Strubbe, D. A.; Fréchet, J. M. J.; Trauner, D.; Louie, S. G.; Crommie, M. F. *Phys. Rev. Lett.* **2007**, *99*, 038301.
- Kumar, A. S.; Ye, T.; Takami, T.; Yu, B.-C.; Flatt, A. K.; Tour, J. M.; Weiss, P. S. *Nano Lett.* **2008**, *8*, 1644.
- Klajn, L. *Pure Appl. Chem.* **2010**, *82*, 2247.
- Gross, H.; Durr, H. *Tetrahedron Lett.* **1981**, *22*, 4679.
- Hauck, G.; Durr, H. *Angew. Chem., Int. Ed. Engl.* **1979**, *18*, 945.
- Love, J. C.; Estroff, L. A.; Kriebel, J. K.; Nuzzo, R. G.; Whitesides, G. M. *Chem. Rev.* **2005**, *105*, 1103.
- Zong, H.; Sun, P.; Mirkin, C. A.; Barrett, A. G. M.; Hoffman, B. M. *J. Phys. Chem. B* **2009**, *113*, 14892.
- Valiokas, R.; Klenkar, G.; Tinazli, A.; Reichel, A.; Tampé, R.; Piehler, J.; Liedberg, B. *Langmuir* **2008**, *24*, 4959.
- Spang, P. Ph.D. Dissertation, 1985.
- Durr, H.; Bouas-Laurent, H. *Photochromism: Molecules and Systems*; Elsevier: Amsterdam, The Netherlands, 1990.
- Crano, J. C.; Guglielmetti, R. J. *Organic Photochromic and Thermochromic Compounds*; Plenum Press: New York, 1999; Vol. 1.
- Durr, H. *Angew. Chem., Int. Ed. Engl.* **1989**, *28*, 413.
- Shrestha, T. B.; Melin, J.; Liu, Y.; Dolgounitcheva, O.; Zakrzewski, V. G.; Pokhrel, M. R.; Goritchiani, E.; Ortiz, J. V.; Turro, C.; Bossman, S. H. *Photochem. Photobiol. Sci.* **2008**, *7*, 1449.
- Hammond, G. S. *J. Am. Chem. Soc.* **1955**, *77*, 334.
- Bartucci, M. A.; Wierzbicki, P. M.; Gwengo, C.; Shajan, S.; Hussain, S. H.; Ciszek, J. W. *Tetrahedron Lett.* **2010**, *51*, 6839.
- Hess, B. A., Jr.; Schaad, L. J. *J. Org. Chem.* **1976**, *41*, 3058.
- Woodward, R. B. *J. Am. Chem. Soc.* **1942**, *64*, 72.
- Jaffé, H. H.; Orchin, M. *Theory and Applications of Ultraviolet Spectroscopy*; John Wiley and Sons, Inc.: New York, 1962.
- Scott, A. I. *Interpretation of the Ultraviolet Spectra of Natural Products*; Pergamon Press Ltd.: New York, 1964.
- Sze, K. H.; Brion, C. E.; Katrib, A.; El-Issa, B. *Chem. Phys.* **1989**, *137*, 369.
- Zou, P.; Strecker, K. E.; Ramirez-Serrano, J.; Jusinski, L. E.; Taathes, C. A.; Osborn, D. L. *Phys. Chem. Chem. Phys.* **2008**, *10*, 713.
- Boldi, A. M.; Anthony, J.; Gramlich, V.; Knobler, C. B.; Boudon, C.; Gisselbrecht, J.-P.; Gross, M.; Diederich, F. *Helv. Chim. Acta* **1995**, *78*, 779.
- Moonen, N. N. P.; Diederich, F. *Org. Biomol. Chem.* **2004**, *2*, 2263.
- Janiak, C. *J. Chem. Soc., Dalton Trans.* **2000**, *21*, 3885.
- Wang, J.; Kulago, A.; Browne, W. R.; Feringa, B. L. *J. Am. Chem. Soc.* **2010**, *132*, 4191.
- Wang, W.; Li, L.-S.; Helms, G.; Zhou, H.-H.; Li, A. D. Q. *J. Am. Chem. Soc.* **2003**, *125*, 1120.
- Bruschi, M.; Giuffreda, M. G.; Lüthi, H. P. *ChemPhysChem* **2005**, *6*, 511.
- Ford, G. P.; Katritzky, A. R.; Topsom, R. D. In *Correlation Analysis in Chemistry*; Chapman, N. B., Shorter, J., Eds.; Plenum Press: New York, 1978; p 269.
- Lin, M. C.; Laidler, K. J. *Can. J. Chem.* **1968**, *46*, 973.
- Dorweiler, C.; Holderbaum, M.; Münzmay, T.; Spang, P.; Dürr, H.; Krüger, C.; Raabe, E. *Chem. Ber.* **1988**, *121*, 843.
- Jönsson, H.-P. Ph.D. Dissertation, 1985.
- Isaacs, N. *Physical Organic Chemistry*, 2 ed.; Wiley and Sons: New York, 1995.
- Penkett, C. S.; Simpson, I. D. *Tetrahedron* **1999**, *55*, 6183.
- Itatani, H.; Bailar, J. C. J. *J. Am. Oil Chem. Soc.* **1967**, *44*, 147.
- Krasnokutskaya, E. A.; Semenischeva, N. I.; Filimonov, V. D.; Knochel, P. *Synthesis* **2007**, *1*, 81.

- (48) Zeidan, T. A.; Kovalenko, S. V.; Manoharan, M.; Clark, R. J.; Ghiviriga, I.; Alabugin, I. V. *J. Am. Chem. Soc.* **2005**, *127*, 4270.
- (49) Feng, Y.-S.; Xie, C.-Q.; Qiao, W.-L.; Xu, H.-J. *Org. Lett.* **2013**, *15*, 936.